A Mobile Indoor Positioning System Founded on Convolutional Extraction of Learned WLAN Fingerprints

Avi Bleiweiss
BShalem Research, Sunnyvale, U.S.A.

Keywords: Indoor Positioning System, WLAN Fingerprint, K-Means Clustering, Convolutional Extraction, KNN.

Abstract: The proliferation of both wireless local area networks and mobile devices facilitated cost-effective indoor positioning systems that obviate the need for expensive infrastructure. We explore a floor-level, indoor localization system to predict the physical position of a mobile device holder in an office space by sensing a fingerprint of signal strength values, received from a plurality of wireless access points. In this work, we devise an instructive model that tailors elemental algorithms for unsupervised fingerprint learning, and resorts to only using a single-layer convolutional neural-network, succeeded by pooling. We applied our model to a fingerprint-based dataset that renders large multi-story buildings, and present a detailed analysis of the effect of changing setup parameters including the number of hidden nodes, the receptive field size, and the stride between extracted features. Our results surprisingly show that classification performance improves markedly with a sparser feature extraction, and affirms a more intuitive gain, yet milder, as any of the number of features or the tile size increases. Despite its simplicity, the positional accuracy we attained is sufficient to provide a useful tool for a location-aware mobile application, purposed to automate the mapping of building occupants.

1 INTRODUCTION

One of the more prominent technologies to provide occupancy information in commercial buildings is Indoor Positioning Systems (IPS). The expansion of location-aware mobile computing to indoors, benefits many real-world consumer applications, including emergency responder, adaptive control of conditioning and lighting, store navigation, and augmented reality. For outdoors, location-based services (LBS) typically utilize Global Positioning Systems (GPS) that provide relatively accurate and robust positioning solution. However, GPS require unobstructed line-of-sight to the orbiting GPS satellites and indoors, its signal becomes substantially compromised and presumed practically unfitting for resolving fine-grain object locations. A variety of alternatives have been proposed for indoor operation ranging from visual through infrared and ultrasound to acoustic (Ruoxi et al., 2014) sensing. Albeit being fairly matured, these techniques are vulnerable to environmental disruptions and therefore require costly custom hardware. On the other hand, the pervasive nature of radio frequency (RF) signals spurred extensive research of IPS founded on wireless networks along with WiFi enabled mobile devices (Ching et al., 2010), to leverage an ever-growing and widespread infrastructure.

In recent years, location fingerprinting methods that harness existed wireless local area network (WLAN) have been proposed for indoor spaces (Kaemarungsi and Krishnamurthy, 2004). Most of WLAN-based positioning systems in indoor environments rest on the Received Signal Strength Indicator (RSSI) measure – the higher the RSSI power level, the better the quality and speed of communications. Typically, WLAN deployment performs a site survey on a rectangular grid of indoor locations to capture RSSI values from a multitude of dispersed wireless access points (WAPs), and obtain maximal space coverage by overlapping transmittance beams. The vector of RSSI intensities associated with each grid point is termed the location fingerprint, and a set of predetermined fingerprints then formalizes a training database that maps all the grid nodes for locality of reference. A mobile device held by an indoor area occupant, captures the signal strengths from all wireless access points, and creates an RSSI vector sample that is further compared to each of the database fingerprints. The position of the person thus corresponds to the location correlated with the most similar fingerprint of the database map (Marques et al., 2012) (Zhou and Shi, 2009). Location accuracy, defined as

Bleiweiss, A.
A Mobile Indoor Positioning System Founded on Convolutional Extraction of Learned WLAN Fingerprints.
DOI: 10.5220/0005685702140223
In *Proceedings of the 5th International Conference on Pattern Recognition Applications and Methods (ICPRAM 2016)*, pages 214-223
ISBN: 978-989-758-173-1

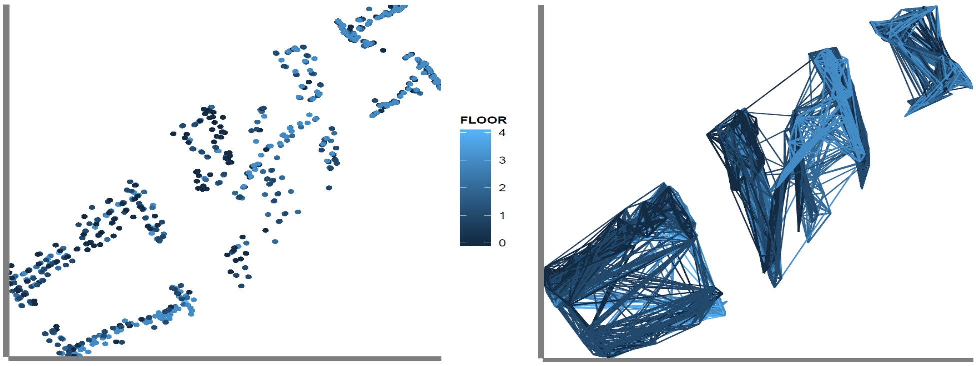

(a) Point spread. (b) Line path.

Figure 1: Physical positional distribution of training data: each mobile device location is expressed in two-dimensional coordinates, shown for each of the floors of the three UJI university buildings in both point spread and line path formations.

the error distance from the actual position, largely depends on the prediction algorithm used and the dataset size (Chen et al., 2006). A real-world application that utilizes a WiFi-based positioning system to track construction site workers, reports a favorable location accuracy of under five meters (Woo et al., 2011).

The fingerprint calibration data collected in an office building is often annotated with a ground-truth location of the mobile device. However, to enable context-aware services that scale well to large wireless infrastructures, mobile devices rather construct their own spatial representation based on sequences of unlabeled RSSI data. This requires the device to simultaneously estimate both its location and the environment mapping (SLAM), corollary to practices in the domain of robotics. To model WiFi signal propagation in space, the work by Ferris et al. (Ferris et al., 2007) is one technique that builds RSSI maps at runtime without resorting to location training labels. By reducing the high dimensional vector of values emanated from all the WAPs in the environment to a two dimensional embedding space, the method facilitates an immediate translation to extract an objective pair of longitude and latitude coordinates of the device.

In our work, we use a pre-compiled SLAM dataset, UJIIndoorLoc, publicly accessible from the UCI Machine Learning Repository (UCI, 2014) and known to date as the largest collection of WiFi fingerprints. UJIIndoorLoc comprises distinct training and validation sets, and is specifically targeted to provide a reference platform for comparing results of independent research that evaluates fingerprint-based indoor localization methodologies. The dataset represents three buildings of the Jaume I University (UJI) campus, each of either four or five floors, with a surface coverage exceeding $10^5 m^2$ (Torres-Sospedra et al., 2014). Figure 1 illustrates the physical positional distribution of the training data collection. Each mobile device location is formulated as a pair of longitude and latitude variables, with occupancy displayed for each of the floors of the three target buildings, and shown in both point spread and line path formations.

A remarkable research effort has been devoted to learning features from unlabeled input data for classification objectives, often typified by deploying increasingly complex algorithms and training a multi-layer of representations, one layer at a time. For analyzing system performance, each of the layers is parameterized by the number of features to learn, the location coordinates of where features are computed, and the designed encoding scheme of system inputs and outputs. In this paper, we explore these parameter choices in seeking higher accuracy rate for predicting a floor-level location of a mobile device indoors, but rather pursue an economical single-layer, convolutional neural-network (CNN) architecture, trained by simple and primitive unsupervised-learning (Duda et al., 2001) methods. Prior work on analyzing single-layer CNN centered primarily on imaging benchmark datasets (Coates et al., 2011), and to the best of our knowledge, the system we propose is the first to incorporate this methodology for evaluating indoor positioning systems. Our proposed solution seamlessly consolidates both information retrieval (Manning et al., 2008) and unsupervised machine learning algorithms, as information retrieval (IR) is rapidly becoming the dominant form of data source access. Our work closely leverages IR practices and follows efficient similarity calculations directly from the well known Vector Space Model (Salton et al., 1975).

Most schemes of feature learning have revolved around single-layer models that are cascaded to build a deeper hierarchy. Typically, the basic building block of a feed-forward CNN alternates between filter banks and a down-sampling layer, and amongst the many modules a CNN is composed of, the unsupervised

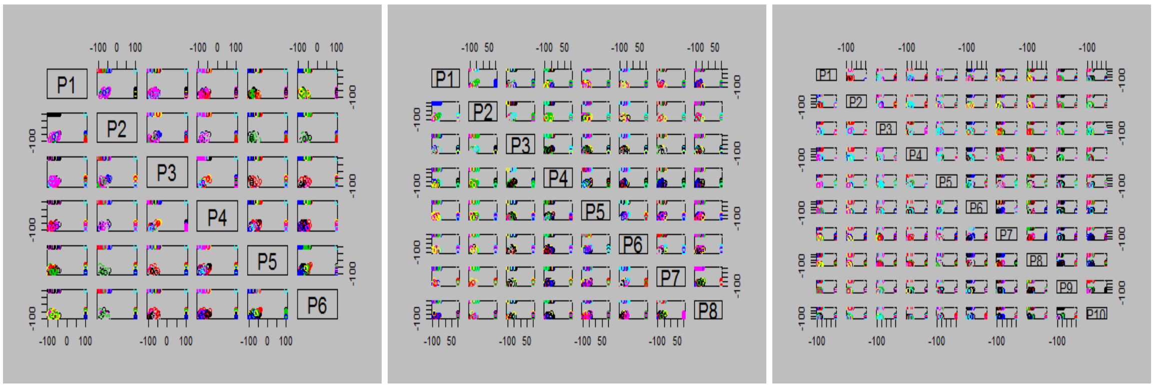

(a) $w = 6$. (b) $w = 8$. (c) $w = 10$.

Figure 2: Visualization of centroids learned by k-means clustering of the UJIIndoorLoc validation set, with 25 randomly selected tiles from each of the unlabeled WiFi fingerprints, and shown for $K = 100$ as a function of the receptive field size, w.

learning algorithm appears to be the most probed. However, recent studies considered the performance impact of other system level parameters that directly affect the design tradeoffs of a CNN architecture, including the number of hidden nodes, the receptive field size, and the sampling stride. The work by Jarrett et al. (Jarrett et al., 2009) proved that introducing non-linearity following the filter banks, produces sparse features that are more suitable for subsequent pooling and shown to be the most single important factor to improve object recognition accuracy. Similarly, over-specifying a larger number of distinctly sampled patches, is the most influential parameter governing visual categorization results (Nowak et al., 2006).

The main contribution of our work is demonstrating that the CNN design considerations we laid out may, in fact, be principal to the algorithm efficacy in learning WiFi fingerprint features for improving the accuracy rate of predicting the floor-level location of a human-held mobile device. Potentially, more important even than the selection of the unsupervised learning algorithm itself. To further commit to this assertion, we use the simple k-means clustering algorithm that requires no tuning parameters and has not been widely adapted for deep feature learning. Surprisingly, our analysis attributes more weight to the choice of feature stride and increased sparsity for ameliorating indoor location prediction, in contrast to the common intuition broadly perceived in the image understanding domain that a denser formulation merits a higher object detection rate. The rest of this paper is organized as follows. In section 2, we describe our feature learning framework that incorporates k-means clustering, coupled with a hard and a soft activation function versions. Section 3 outlines the process flow of fingerprint feature extraction prescribed in a parameterized single-layer CNN architecture, leading to our majority-voting based k-nearest neighbor, baseline classification method. We then present our evaluation methodology for analyzing WiFi fingerprinting in using the UJIIndoorLoc (UCI, 2014) dataset, and report extensive quantitative results of our experiments, in section 4. We conclude with a discussion and future prospect remarks in section 5.

2 FINGERPRINT LEARNING

In our feature learning framework, we view the dataset of WiFi fingerprint vectors as a matrix $W \in \mathbb{R}^{mxn}$, where m are the distinct, indoor mobile-device locations, and n the RSSI measurements captured from all the WAPs in all the site buildings. We then define a fingerprint tile as a contiguous subset of a fingerprint vector with a dimension w and of d channels. Conventionally, w is referred to as the receptive field size and for fingerprint data, d is fixed and set to one. Each fingerprint tile is then represented as a vector $x \in \mathbb{R}^N$ of RSSI intensity values, where $N = w \cdot d$.

Our fingerprint learning process proceeds in several stages. First, we extract random tiles from unlabeled training fingerprints and construct a dataset of l randomly sampled tiles $X = \{x^{(1)}, x^{(2)}, ..., x^{(l)}\}$, where $x^{(i)} \in \mathbb{R}^N$. Then, every tile, $x^{(i)}$, is optionally normalized by subtracting the mean and dividing by the standard deviation of the tile vector elements. After tile normalization, to discover features (Rajaraman and Ullman, 2011) from unlabeled WiFi fingerprint data, we employ the exceptionally efficient and simple to tune k-means clustering algorithm that is used extensively in the domain of computer vision. The k-means unsupervised learning procedure takes the dataset X and produces a function $f : \mathbb{R}^N \rightarrow \mathbb{R}^K$ that maps an input tile vector $x^{(i)}$ to a new feature vector of K dimensionality, where K is an algorithm control parameter that sets the number of clusters to generate, and the k^{th} feature of the mapped vector is denoted as f_k. The k-means algorithm uses the Euclidean distance measure and learns K centroids, $c^{(k)}$, from the input tiled data, X. Figure 2 provides visualization of bases, or centroids, learned by k-means clustering of the UJI-IndoorLoc validation set, with 25 randomly selected tiles from each of the unlabeled WiFi fingerprints, and shown for $K = 100$ as a function of an increased receptive field size, w. We consider two versions of the feature mapping function f (Coates et al., 2011). A standard 1-of-K, hard assignment encoding scheme

$$f_k(x) = \begin{cases} 1 & \text{if } k = argmin_j \|c^{(j)} - x\|_2^2 \\ 0 & \text{otherwise,} \end{cases} \tag{1}$$

and a non-linear soft mapping that offers a sparse output, more suitable to the CNN pooling stage, and is governed by the following equation

$$f_k(x) = max\{0, \mu(z) - z_k\}, \tag{2}$$

where $z_k = \|x - c^{(k)}\|_2$ and $\mu(z)$ is the mean of the elements of z. Function f transforms an input tile $x \in \mathbb{R}^N$ to a new representation $y = f(x) \in \mathbb{R}^K$ that we use as a learned feature extractor and apply it to our labeled training fingerprints, for classification. Hereon, to tell them apart, the activation functions are referred to as k-means hard and k-means soft, respectively.

3 CNN EXTRACTION

In this step, we extract features from equally spaced tiles that cover an entire input fingerprint vector of the labeled training dataset, and further reduce layer dimensionality by pooling features together over specified regions. We apply either the hard or the soft version of our k-means feature extractor, $f : \mathbb{R}^N \to \mathbb{R}^K$, to a multitude of fingerprint tiles, each of length w, and compute a compact representation $y \in \mathbb{R}^K$ for each tile. The definition of a single layer architecture for convolutional fingerprint extraction ensues by deploying the function f to any number of tiles, uniformly selected from the entire scope of an input fingerprint vector. This process is graphically staged in Figure 3. Distinctly, given a single channel, WiFi fingerprint vector of n RSSI intensity elements, construed as tiles of a receptive field size w each, and are evenly spaced by a stride s of signal strength values, we formalize the interpretation y as $(\frac{(n-w)}{s} + 1)$, K-dimensional feature vectors, each computed for a fingerprint tile.

The extracted feature vectors, $y^{(i)}$, are successively pooled over two evenly sized half-space bins by computing the sum of all the $y^{(i)}$ contributing in each region, to form the feature vector Φ of dimensionality $2K$ that we use for classification. Given t, the number of tile samples in a fingerprint of size n, then the relationship $t \cdot K \gg n$ often holds to justify pooling for dimensionality reduction of features, a key step to merit efficient classification computation. To our pooled, $2K$-dimensional feature vectors, $\Phi^{(i)}$, constructed for each training WiFi fingerprint and a label, we apply a majority-voting based k-nearest neighbor (Cormen et al., 1990), baseline classifier to evaluate our system cross-validation accuracy for predicting floor-level indoor location of a mobile device.

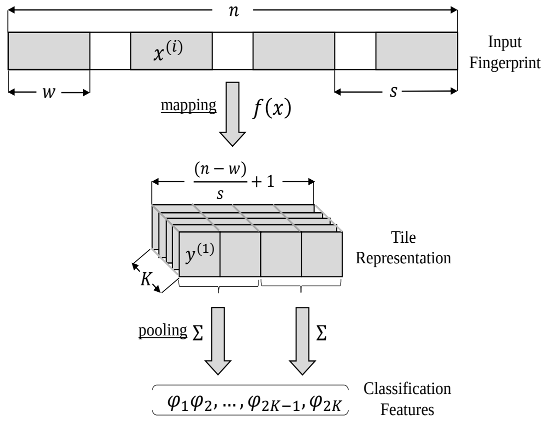

Figure 3: Convolutional feature extraction using a receptive field size w and a stride s. Evenly distributed WiFi tiles, $x^{(i)}$, of the input fingerprint vector of n RSSI intensity components, are mapped to K-dimensional feature vectors to form a new fingerprint interpretation. Following a standard practice in deep feature learning, the mapped vectors are then sum-pooled over a half-space local region to derive a feature vector Φ of dimensionality $2K$, we further use for classification. For clarity, the stride shown for the input fingerprint vector is greater than the receptive field size, but in practice, the step s is almost always smaller than w.

4 EMPIRICAL EVALUATION

To validate our system in practice, we have implemented a software library that realizes the analysis of WiFi fingerprinting in several stages. After collecting and cleaning the archived indoor data, we learn unlabeled fingerprints by performing k-means clustering (Kaufman and Rousseeuw, 1990) on randomly selected tiles drawn from the validation dataset. Using a single-layer CNN architecture, we then extract features from labeled training fingerprints for classification. Our learning framework behavior is primarily governed by the setting of the number of features, K, the receptive field size, w, and the stride, s. We report our experimental results on the impact of modifying

Table 1: Positional distribution of humanly held mobile devices, broken down by individual floors of each of the experimented UJI campus buildings, for both the training and validation subsets. NA signifies a non-existent fifth floor in a building.

Dataset	Building	1^{st} Floor	2^{nd} Floor	3^{rd} Floor	4^{th} Floor	5^{th} Floor	Total	Mean	SD
Training	1	1059	1356	1443	1391	NA	5249	1049.8	172.6
	2	1368	1484	1396	948	NA	5196	1039.2	239.1
	3	1942	2162	1577	2709	1102	9492	1898.4	605.4
Validation	1	78	208	165	85	NA	536	134	63.2
	2	30	143	87	47	NA	307	76.8	50.2
	3	24	111	54	40	39	268	53.6	33.8

these parameters by performing cross-validation.

4.1 Experimental Setup

Our work exploits the R programming language (R, 1997) to acquire the raw UJIIndoorLoc dataset from the UCI Machine Learning Repository (UCI, 2014), and fosters cleanup to serve useful in our software environment. The extensive WiFi fingerprint dataset, purposed to evaluate indoor positioning systems, is multivariate and every row of the data frame comprises 529 columns that coalesce features of different categories, each represented as a vector, possibly combining real, integer, and boolean element types. A set of intensity values leads off to form the WiFi fingerprint vector. A fingerprint is described by 520 integer elements, each spans the $[-104, 0]$ decibel-milliwatts (dBm) range, corresponding to the weakest ($-104dBm$) and exceptionally strong ($0dBm$) signal when contributed by a discovered wireless access point, or set uniformly to $+100dBm$ to indicate an undetected WAP. Individual RSSI measurements both inside $[-45dBm, 0dBm]$ and under $-95dBm$ are rare and retain inconsequential percentage of the total intensity values captured (Torres-Sospedra et al., 2014).

Each fingerprint rendition follows with an associated set of six real-world device location properties, to be either partially or in its entirety predicted in the classification process. This output label vector comprises three-dimensional positional coordinates including longitude and latitude that are measured in meters and reference the Universal Transverse Mercator (UTM) grid, and an altitude value designated by the floor enumeration in a building $\in [0, 4]$. Along with relational space identifiers that further expand the fingerprint physical position and incorporate the building id $\in [0, 2]$, a categorical definition of the indoor closed area that encompasses the wireless trace e.g. a classroom, a lab, or an office, and a location proximity indicator denoting the held device of being either inside the specified region or outside and right in front of the door of the prescribed space perimeter.

Lastly, a global class of attributes correlate user and mobile device information to the acquired fingerprint data, and in addition provides an accurate and device independent time-stamp for the WiFi recording that took place. Eighteen individuals in total, user id $\in [1, 18]$, participated in the process of collecting the training samples, each identified by a physical height that is dereferenced via a separate table. This adds a fine-grained, spatial positional dimension to the device, found to directly impact its RSSI readings (Kaemarungsi and Krishnamurthy, 2004). Mobile device wise, twenty unique phone models, populated with twenty five distinct Android OS versions, were deployed to obtain the fingerprint data. As a three dimensional table facilitates the essential mapping from an itemized device list onto a phone model, the installed system-image version, and the associated user enumeration. User id 0 is uniquely assigned for capturing the validation fingerprint collection and its occurrences relate several different phone models.

Quantitatively, the UJIIndoorLoc dataset is split into a training subset of 19,937 fingerprint instances, and an exclusive validation part of 1,111 WiFi recordings. Training held-device locations regularly correspond to pre-defined reference points, whereas validation wireless readings were gathered from arbitrary coordinates inside the buildings, without performing any user tracking to better emulate a real-world indoor positioning system. Notably, the validation collection has several fields intentionally unlabeled in each of its records, including the affiliated closed space and user properties. Table 1 shows positional distribution of humanly held mobile devices, broken down by individual floors of each of the targeted UJI campus buildings, for both the training and validation subsets. The first and the second subject buildings are each of four floors with more evenly spread training fingerprints, as the third building has five stories and exposes a

Table 2: Unique RSSI values presented in a fingerprint tile dataset, X_i,shown as a function of increased receptive field size.

Receptive Field Size	2	4	6	8	10	12	14	16	18
Unique Fingerprints	341	927	1506	2110	2664	3194	3737	4171	4620

higher standard deviation. For this study, we are primarily interested in the system performance of classifying floor-level device location, hence longitude, latitude, and space properties of the output feature vector are unsubstantiated. Similarly, analysis related to user and device attributes is outside the scope of our current implementation and is deferred to future work.

4.2 Experimental Results

In this section we report experimental results of evaluating our indoor positioning system, using the UJIIndoorLoc validation subset to cross-validate its training companion. Our testing methodology commences by training unnormalized WiFi fingerprints in a single layer CNN, employing both the hard and soft versions of the k-means feature mapping function f, as we vary our system parameters K, w, and s. We then train a baseline k-nearest neighbor (KNN) classifier and test it on the validation set. In KNN, we compute the Euclidean-squared distance between a validation-fingerprint mapped vector against each learned training vector. Our selected $k = 10$ most nearest training samples are sorted in a non-descending order, and by a majority rule we derive a score for all the building-floor pairs. This score is further accumulated and averaged across validation fingerprints, singled out for each of the building-floor pairs, and the matching pair corresponds then to the highest average scoring. Our experiments ascribe a discrete value set to each of our model parameters, K, w, and s. Respectively, we use representations of 10, 25, 50, 100, and 250 learned features, a series of receptive field sizes $\in [2,18]$ in increments of two, and stride values of 1, 2, 4 and 8.

A close observation at the validation raw fingerprints reveals a highly sparse data structure with a fairly large proportion of about 91% of vector elements are assigned the value of $+100dBm$, signifying many wireless access points are undiscovered at the designated device locations. This review warranted the generation of many thousands of fingerprint tiles to challenge the dispersed WiFi feature data, and ensure that k-means produces statistically reasoned clusters. Hence, in learning our fingerprint feature representation, for every system setting of the receptive field size we sampled 25 random tiles from each of the RSSI recording vectors of the unlabeled validation set, and constructed our collection of tile datasets, X_i, where $i \in 1,2,...,T$, and $T = 9$, the number of system choices for setting w. For 1,111 WiFi fingerprints, this yielded per dataset a total of 27,775 tiles to learn their centroids from, each with a corresponding dimensionality of the specified receptive field size. From an alternate perspective, the uniqueness of values obtained from WiFi signal measurements in a tile dataset, X_i, is also vital to clustering robustness. Table 2 depicts the number of distinct RSSI vectors in each of the designated tile datasets, X_i, as a function of our experimental set of receptive field sizes, shown in a non-descending order. Given our discrete choices for varying the number of features, K, we hereon report our results using receptive field sizes that are greater than four, with no less than 1,500 differentiable tiles.

For succinctness, we use the compact notation $\lambda(K,w,s)$ to describe our parametrically driven, IPS implementation model that exploits a single layer CNN. Using the UJIIndoorLoc validation dataset, we evaluate our system for floor-level device location pairing, by only varying one model parameter at a time, while keeping the other two variables uniformly constant and assigned to a prescribed default value.

First, we modified the number of features, or centroids, K, in conjunction with fixing the receptive field size to six RSSI length, and setting the feature extracting spacing between fingerprint tiles to one, generally considered optimal for convolutional learning systems. However, systems for learning features from two dimensional images use a stride $s > 1$ to step across patches and avoid excessive computational cost. In contrast, for the WiFi fingerprint data, traversing the tiles is of a considerably reduced linear time complexity, and lets us strike a more reasonable balance between process running time and algorithm robustness. Figure 4(a) and Figure 5(a) show the effect on system average accuracy as the experimentally prescribed, number of learned centroids increases, applying both the hard and soft versions of the k-means activation function, f, respectively. For visualization conciseness, positional performance is categorized by the subject building id, rather than by each and every pair of building and floor combinations. In learning more centroids, the soft algorithm attains higher positional accuracy almost consistently for all the three buildings. The mild performance decline observed for $K = 250$ is mostly attributed to constraint clustering due to our highly sparse tiling datasets. On the other hand, k-means hard performed as expected for

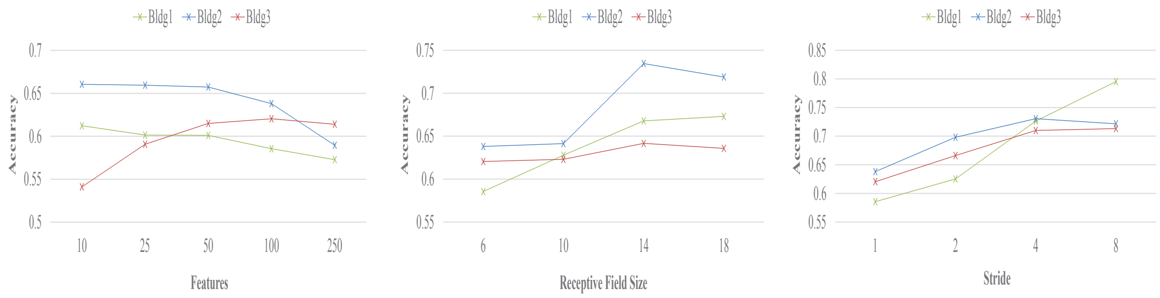

(a) Number of features, K. (b) Receptive field size, w. (c) Stride, s.

Figure 4: Floor-level, system average accuracy using the hard k-means feature mapping function. Shown for varying each of the model governing parameters, (K, w, s), and each categorized by the subject building id.

(a) Number of features, K. (b) Receptive field size, w. (c) Stride, s.

Figure 5: Floor-level, system average accuracy using the soft k-means feature mapping function. Shown for varying each of the model governing parameters, (K, w, s), and each categorized by the subject building id.

the third building, but rather exposes an inconsistent accuracy drop for both building ids, one and two. Notably, the 3^{rd} building occupies five floors and owns almost half of the training fingerprint data (Table 1).

Next, we stepped discretely along the second axis of our learning model, $\lambda(K,w,s)$, and quantified the related incremental effect on our floor-level, positional classification rate. We sought after leveraging the k-means algorithm to learn larger receptive fields and possibly reduce feature sparseness in a tile that overlaps an enlarged extent of a raw WiFi fingerprint. Clearly, this necessitates an expansion of the state space for the learning algorithm to operate on, and thereof mandates an increased number of features to learn. For this experiment, we tried receptive field sizes of 6, 10, 14, and 18 to ensure the tile datasets are of the highest distinctive wireless recordings. We held the stride to one RSSI length, and selected a reasonably high count of 100 centroids. An overview of our performance results for both the hard and soft versions of our k-means feature mapping is shown in Figure 4(b) and Figure 5(b), respectively. Both variants of f behave almost identically, though the soft version is more modestly stable, and trend towards elevating location matching accuracy as the receptive field size increases, with the exception of the third target building that displays a relatively flat performance.

Lastly, we evaluated the impact of altering the stride parameter, s, on predicting the indoor location of a humanly held, mobile device. For this experiment we varied the stride over 1, 2, 4, and 8 consecutive RSSI elements, fixed the number of centroids to learn to 100, and set the receptive field size w to 6. The summary of our performance results for both the hard and soft versions of our activation function, f, is shown in Figure 4(c) and Figure 5(c), respectively. Surprisingly, our results challenge a basic intuition that despite an apparent reduction of the tile sampling rate, we rather demonstrate a striking upward accuracy trend as we increase the step size between fingerprint tiles. Indifferent to the mapping function form, floor-level accuracy for building one, for example, depicts a marked climb from 0.58 to 0.79, or a 36% gain, as the stride treads a full extent from 1 to 8 RSSI units. In contrast to a much milder performance gain observed when varying any of the centroid count or the receptive field size, model parameters.

In addition to reporting average accuracy per subject building, we were interested in evaluating our absolute system performance of device positional matching for the broader and finer composition set of all the possible building-floor pairs, p_{br}, where

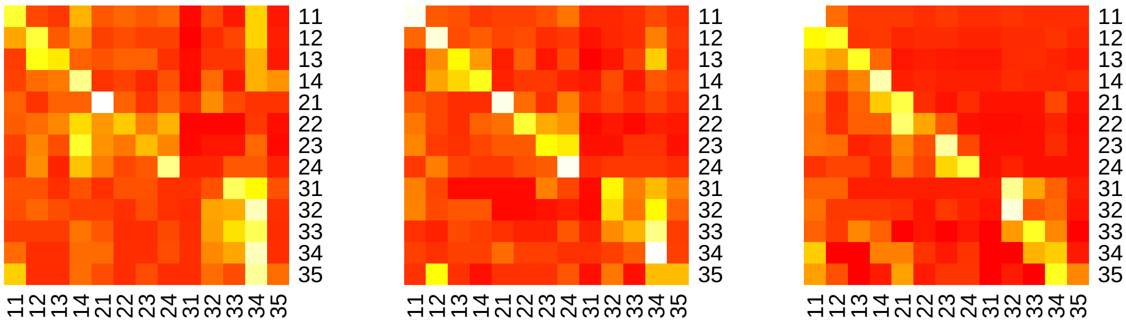

(a) $K = 100, w = 6, s = 1$. (b) $K = 100, w = 14, s = 1$. (c) $K = 100, w = 6, s = 8$.

Figure 6: Confusion matrices for all the valid thirteen building-floor combination pairs, using k-means hard learning with preferred model parameters, (K, w, s).

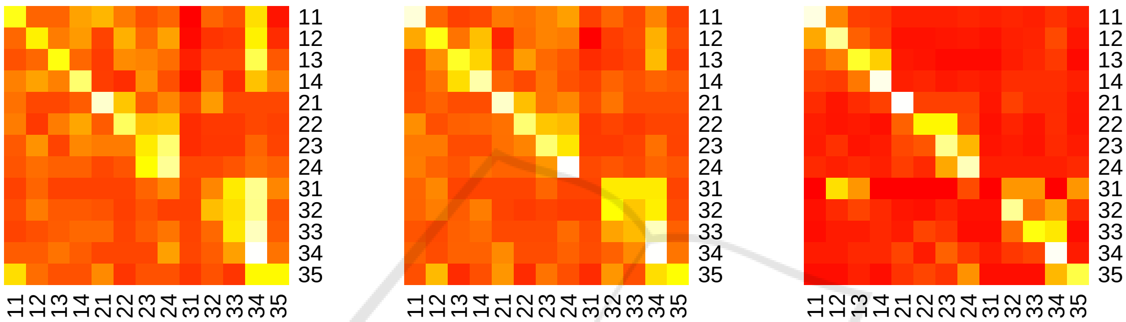

(a) $K = 100, w = 6, s = 1$. (b) $K = 100, w = 14, s = 1$. (c) $K = 100, w = 6, s = 8$.

Figure 7: Confusion matrices for all the valid thirteen building-floor combination pairs, using k-means soft learning with preferred model parameters, (K, w, s).

$1 \leq b \leq 3$ and $1 \leq r \leq 5$, excluding the non-existent p_{15} and p_{25} pairing choices, as prescribed by the UJI-IndoorLoc dataset. Figure 6 and Figure 7 depict confusion matrices for all predicted against actual thirteen building-floor combination pairs, p_{br}, assessing both the hard and soft designs of the feature mapping function, f, respectively. As the parameters of our learning model, $\lambda(K, w, s)$, are fixed to a limited set of preferred values we obtained from analyzing our building scoped performance data. Evidently, results for stride $s = 8$ are by far the better achieving with a slight edge towards the soft activation version.

Selecting a set of model parameters entails thereof a location-pairing accuracy tradeoff, we further quantify against the implied computational cost. Figure 8 shows the normalized running time of feature learning, as we vary each of the governing parameters, (K, w, s), and respectively contrasting the hard with the soft k-means mapping functions. Execution time tends to rise fairly close to linear as the number of centroids to learn increases, whereas a local minimum is evident for $w = 14$ and immediately thereafter a steep non-linear leap, as we step through the experimental receptive field sizes. Incrementing the stride, s, consistently trends a notable commensurate decline of running time. Overall, and as expected, the soft feature mapping tracks well the hard version behavior, albeit running slower and at a proportional scale.

5 CONCLUSIONS

We have demonstrated the apparent potential in deploying a learning architecture comprised of a single convolutional layer for extracting WiFi fingerprint features, to predict floor-level position of a human-held mobile device, indoors. We conducted extensive experiments using the recently introduced UJI-IndoorLoc dataset, and assessed the effect of varying neural-network parameters on location matching accuracy. Despite an extremely simple learning algorithm, k-means clustering, each of the model controls we tested including centroid count, receptive field size, and stride, conferred either a milder or a significant impact on our system classification performance.

One of the major challenges of our work was the highly sparse context of the WiFi fingerprint tiles with a majority of undetected, wireless access points. Con-

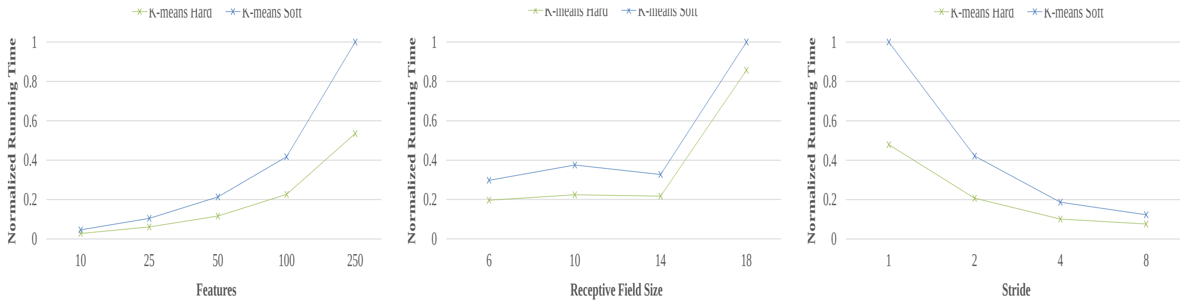

(a) Number of features, K. (b) Receptive field size, w. (c) Stride, s.

Figure 8: Normalized compute running time of feature learning. Shown for varying each of the model governing parameters, (K, w, s), and respectively contrasting the hard with soft k-means activation functions.

sequently, some of the more ubiquitous and essential intuitions that more centroids to learn and denser feature extraction benefit performance greatly, become considerably unsubstantiated. While confirming that more features and larger receptive field size conclude in a relative benign performance gain, the most surprising result of our work is the striking behavior of ascending positional accuracy as the sampling of the fingerprint tiles becomes coarser, by increasing the stride parameter. This result may seem inexplicable at first observation, but the larger stride is likely to sample more unique RSSI values to avoid underfitting, and hence the improved location identification. Respectively, sparse sampling also merits a proportional decline in system-level computational cost.

To the best of our knowledge, and based on literature published to date, we are unaware of indoor positional systems with similar goals to evenhandedly contrast our results against. The creators of the UJI-IndoorLoc dataset (Torres-Sospedra et al., 2014) have provided a basic reference implementation of an IPS that employs a Euclidean distance based KNN classifier with $k = 1$. The classifier operates on the original unpacked WiFi fingerprints of 520 elements each, drawn out directly from the database. Unlike our system that commences by performing convolutional feature extraction, and utilizes pooling to produce an $O(n/K)$ compact tile representation of much reduced dimensionality that is used subsequently for classification. Assuming that performing CNN feature learning is a rather infrequent event in our pipeline, our classification phase is presumably more efficient computationally, and furthermore it scales well to large WiFi infrastructures of thousands of wireless access points and tens of thousands fingerprint records. For cross-validation, the reference implementation reports a success rate of %89.9 for correctly identifying a fingerprint location in a building-floor pairing. Despite our fairly rigorous pooling scheme, to predict an identical positional target, we recorded a respectful 0.79 accuracy of floor-level location matching, for a sparse tile sampling with a stride $s = 8$.

A direct progression of our work is to evolve our positioning system to ultimately predict the finer, user location components of longitude and latitude in conjunction with the third dimension of the floor enumeration in the target building. Similarly, we find a useful value-add in extending our work to better understand the implications of the user height and the mobile device type on our overall, system performance rate. Given the limited vocabulary of RSSI values, exploring a bag of words (Baeza-Yates and Ribeiro-Neto, 1999) format for a more compact fingerprint representation, holds the prospect to ameliorate overall compute efficiency. We look forward to advance our study and incorporate a more adaptive sampling of the fingerprint tile data for feature extraction, rather than using a uniform stride, and further improve our system accuracy. Incorporating a more comprehensive linear-SVM classifier, as an additional option to our baseline KNN model that is exclusively trained on a single parameter k, is pertinent to our work to possibly enhance positional matching performance.

We hope that this work and others to follow, will provide researchers a larger foundation for comparing results of different learning algorithms that key off an identical, indoor location dataset.

ACKNOWLEDGEMENTS

We would like to thank the anonymous reviewers for their insightful suggestions and feedback.

REFERENCES

Baeza-Yates, R. and Ribeiro-Neto, B., editors (1999). *Modern Information Retrieval*. ACM Press Series/Addison Wesley, Essex, UK.

Chen, M. Y., Sohn, T., Chmelev, D., Haehnel, D., Hightower, J., Hughes, J., LaMarca, A., Potter, F., Smith, I., and Varshavsky, A. (2006). Practical metropolitan-scale positioning for GSM phones. In *Ubiquitous Computing (UbiComp)*, pages 225–242, Orange County, CA.

Ching, W., Rue, J. T., Binghao, L., and Rizos, C. (2010). Uniwide WiFi based positioning system. In *Technology and Society (ISTAS)*, pages 180–189, Wollongong, Australia.

Coates, A., Lee, H., and Ng, A. (2011). An analysis of single-layer networks in unsupervised feature learning. In *JMLR Artificial Intelligence and Statistics*, pages 215–223, Fort Lauderdale, FL.

Cormen, T. H., Leiserson, C. H., Rivest, R. L., and Stein, C. (1990). *Introduction to Algorithms*. MIT Press/McGraw-Hill Book Company, Cambridge, MA.

Duda, R. O., Hart, P. E., and Stork, D. G. (2001). Unsupervised learning and clustering. In *Pattern Classification*, pages 517–601. Wiley, New York, NY.

Ferris, B., Fox, D., and Lawrence, N. D. (2007). WiFi-SLAM using gaussian process latent variable models. In *International Joint Conference on Artificial Intelligence (IJCAI)*, pages 2480–2485, Hyderabad, India.

Jarrett, K., Kavukcuoglu, K., Ranzato, M., and LeCun, Y. (2009). What is the best multi-stage architecture for object recognition? In *International Conference on Computer Vision (ICCV)*, pages 2146–2153, Kyoto, Japan.

Kaemarungsi, K. and Krishnamurthy, P. (2004). Modeling of indoor positioning systems based on location fingerprinting. In *IEEE Computer and Communication Societies (INFOCOM)*, pages 1012–1022, Hong Kong.

Kaufman, L. and Rousseeuw, P. J., editors (1990). *Finding Groups in Data: An Introduction to Cluster Analysis*. Wiley, New York, NY.

Manning, C. D., Raghavan, P., and Schutze, H. (2008). *Introduction to Information Retrieval*. Cambridge University Press, Cambridge, United Kingdom.

Marques, N., Meneses, F., and Moreira, A. (2012). Combining similarity functions and majority rules for multi-building, multi-floor, WiFi positioning. In *Indoor Positioning and Indoor Navigation (IPIN)*, pages 1–9, Sydney, Australia.

Nowak, E., Jurie, F., and Triggs, B. (2006). Sampling strategies for bag-of-features image classification. In *European Conference on Computer Vision (ECCV)*, pages 490–503, Graz, Austria.

R (1997). R project for statistical computing. http://www.r-project.org/.

Rajaraman, R. and Ullman, J. D. (2011). *Mining of Massive Datasets*. Cambridge University Press, New York, NY.

Ruoxi, J., Ming, J., and Costas, J. S. (2014). Sound-Loc: Acoustic method for indoor localization without infrastructure. *Computing Research Repository, Human-Computer Interaction*, arXiv:1407.4409. http://arxiv.org/abs/1407.4409.

Salton, G., Wong, A., and Yang, C. S. (1975). A vector space model for automatic indexing. *Communications of the ACM*, 18(11):613–620.

Torres-Sospedra, J., Montoliu, R., Martinez-Uso, A., Arnau, T. J., Avariento, J. P., Benedito-Bordonau, M., and Huerta, J. (2014). UJIIndoorLoc: A new multi-building and multi-floor database for WLAN fingerprint-based indoor localization problems. In *Indoor Positioning and Indoor Navigation (IPIN)*, Busan, Korea.

UCI (2014). Machine learning repository - UJIIndoorLoc data set. http://archive.ics.uci.edu/ml/datasets/UJIIndoorLoc.

Woo, S., Jeong, S., Mok, E., Xia, L., Choi, C., Pyeon, M., and Heo, J. (2011). Application of WiFi-based indoor positioning system for labor tracking at construction sites: A case study in Guangzhou MTR. *Automation in Construction*, 20(1):3–13.

Zhou, J. and Shi, J. (2009). RFID localization algorithms and application: a review. *Journal of Intelligent Manufacturing*, 20(6):695–707.